JOINT EUROPEAN TORUS JET

JET–P(890)05

J.P. Christiansen, J.G. Cordey and K. Thomsen

A Unified Physical Scaling Law for Tokomak Energy Confinement

A Unified Physical Scaling Law for Tokomak Energy Confinement

J.P. Christiansen, J.G. Cordey and K. Thomsen

JET-Joint Undertaking, Culham Science Centre, OX14 3DB, Abingdon, UK

** See Appendix 1*

Preprint of Paper to be submitted for publication in
Nuclear Fusion

A unified physical scaling law for Tokamak energy confinement

J. P. Christiansen, J. G. Cordey, K. Thomsen
JET Joint Undertaking, Abingdon OX14 3EA

Abstract

From the equations which describe local transport in a turbulent plasma the scaling of the local diffusivity with the plasma parameters may be established. By appropriate choices of time and length scales for the turbulence it is shown that the scaling of the global energy confinement can be cast in two limiting forms: a short and a long wavelength scaling. The scaling laws consist of a leading term and a function F whose arguments are the dimensionless normalised plasma collisionality and beta. The scaling of the leading term in the short wavelength expression for global confinement is shown to fit both JET L and H-mode confinement data. The function F which describes the precise physical mechanism of the turbulence is found to increase with collisionality but its dependence on the plasma beta remains uncertain. Several theoretical models are found to be a reasonable fit to the JET confinement data, however others such as DTEM can be discarded. The short wavelength confinement scaling is shown to unify a multiplicity of existing theoretical-empirical scaling laws by suitable choices of the function F. These scaling laws all exhibit a similar dependence of F upon collisionality but have different dependencies upon the plasma β . It is shown that for the JET data it is very difficult to determine the β dependence and this explains why so many apparently different scaling laws produce reasonable fits to the data. Using the leading term of the scaling, the fusion product can be extrapolated to reactor conditions (ITER) with an uncertainty factor of 4. This uncertainty can be reduced to $\pm$ 30% by the use of a similarity technique in which F is determined directly from the JET data.

1. Introduction

The scaling of plasma confinement in a Tokamak has been studied extensively since the first scaling law was determined from T-3 [1] nearly twenty years ago. The review article by Hugill [2] surveys the scaling in ohmically heated Tokamaks and in references [3] and [4] ohmic data from various Tokamak devices have been used to establish empirical laws for scaling with geometry, field, current etc. through inter-machine comparisons of data. From

studies of data on Tokamaks with additional heating, neutral beam heating (NBI), ion cyclotron resonance heating (ICRH), electron cyclotron resonance heating (ECRH), a large number of empirical scaling laws has been established. Most of the scaling laws listed separately in references [5-18] will be examined in this paper. These scaling laws have been derived by analysis of data obtained on such Tokamak experiments as PLT, PDX, DITE, DIII, T-10, Alcator, ASDEX, JFT-2M and the larger experiments TFTR, DIII-D, JT-60 and JET.

The anomalous transport observed in Tokamaks has been the subject of many theoretical studies. Transport theories are based on the non-linear saturated state of plasma instabilities but so far no single theory has emerged to explain the variety of phenomena that are observed experimentally. All theoretically plausible scalings for transport in a Tokamak plasma must satisfy certain physical constraints and be expressable in terms of dimensionless parameters [10,19]. Such parameters with their physical interpretation can be derived from the transport equations using the Connor-Taylor invariance approach [20]. The work in this field has recently been reviewed by Connor [21]; this paper presents a complete survey of the constraints imposed on the form of the local thermal diffusivity by various theoretical models of plasma transport. Reference [21] together with references [5-18] and JET data form the basis of the work presented in this paper.

The starting point is the representation of a local thermal diffusivity χ in a dimensionally correct form. Most of the plausible theories for anomalous transport in a Tokamak are characterized by plasma turbulence with frequencies $\omega \ll \Omega_{ci}$ (ion cyclotron frequency) and a short wavelength cut-off $\lambda \gg \lambda_{Debye}$. The long wavelength cut-off is theoretically less certain. Thus two limits are considered : i) a short wavelength limit with $\lambda \sim \rho$ (a Larmor radius) and ii) a long wavelength limit with $\lambda \sim$ L (large scale length like minor radius). In section 2 we show that for both limits the local diffusivity χ scales as the product of a leading term and a function F whose arguments are dimensionless local parameters. Theoretically the function F is specified only when a physical mechanism for thermal transport is chosen, e.g. some type of instability. The leading term in the short wavelength limit exhibits the "gyro-reduced Bohm" scaling while the long wavelength limit corresponds to Bohm scaling. Both limits for χ are shown to yield scalings for the confinement time τ_E in terms of volume average plasma density n, toroidal current I, input power P, minor-major radius a-R, elongation κ, and a function F of global dimensionless parameters. The dependence of τ_E on F is weaker than the dependence of χ upon F ; this makes it more difficult to determine F from global data. F depends on dimensionless parameters like collisionality ν_*, plasma beta β and ratios between characteristic scale lengths such as aspect ratio $\varepsilon = a/R$. Both confinement scalings are applied to JET data in section 3 and we demonstrate that the short wavelength leading term can explain more than one order of magnitude variation in JET confinement

properties; the long wavelength leading term gives a poorer fit to the data. The spread of data around the short wavelength scaling is mainly due to the variation of the function F with ν_*. In section 4 it is shown that F increases with collisionality ν_* which in JET experiments has been varied by more than four orders of magnitude. The analysis of the variation of F with β is impeded by the lack of variation of β in the data for JET (only a factor 10) and it has not been possible to draw any firm conclusions about the β dependence in the confinement data as noted in [10].

The first main result of our work is the identification of the leading term in global confinement scaling as being that associated with the gyro-reduced Bohm scaling of diffusivity.

The second result is that from the global confinement data we can determine the functional dependence of F upon ν_* while the dependence on β remains uncertain. Section 4 shows that various theoretical models for transport caused by instabilities such as the η_i mode, the resistive ballooning mode or collisional drift waves can equally well fit JET data; however some theoretical models e.g. the dissipative trapped electron mode (DTEM), can be discarded on the grounds that they do not exhibit the scaling with collisionality seen in the data.

The third result of our work is described in section 5. We show how a multiplicity of existing scaling laws [5-18] can be transformed to the gyro-reduced Bohm form by appropriate choices of the function F. The transformation demonstrates that most existing scaling laws feature the same dependence upon collisionality ν^* which is observed in the JET data. On the other hand the scaling laws are found to have different dependencies upon β. This together with the uncertainty of the β dependence in the data explains why a variety of scaling laws give a reasonably fit to the confinement data in JET and other Tokamaks.

For ohmically heated plasmas the ohmic heating constraint further restricts the functional dependence of τ_E and the stored thermal energy W. Since it is difficult to accurately determine the ohmic heating rate, we simply demonstrate in section 6 that the measured stored energy W obeys the short wavelength scaling.

A fourth result of our work is that the fusion product $nT\tau_E$, where T is the plasma temperature, can be extrapolated by the gyro-reduced Bohm scaling to reactor conditions with an uncertainty of a factor 4. Section 7 shows that this factor can be further reduced if the collisionality ν_* and β remain fixed in the extrapolation i.e. by using a similarity technique to determine F from existing data. The representations of the off-set linear and the power laws for τ_E and the L and H-mode confinement regimes are all contained in the function F. The similarity technique thus avoids the need to distinguish between these representations.

In this paper we use a standard notation : subscripts i and e refer to ions and electrons; W is the total stored thermal plasma energy which excludes the fast ion energy due to additional heating; P describes the total input power $P = P_{OH} + P_{NBI} + P_{ICRH} - \frac{dW}{dt}$. SI units are used with temperatures in eV.

2. The leading term in Tokamak scaling laws

Global plasma confinement may be dependent upon more than one single physics process. Models for Tokamak transport [22-24] have allowed for different transport scalings within different radial zones, e.g. sawtooth region, confinement region, edge region. The scaling of χ with various plasma parameters such as density n, temperature T, magnetic field B etc. may therefore differ from one region to the next. The scaling of the energy confinement time results from a *convolution* of the scaling of χ in the various regions. From reference [25] the convolution can formally be expressed as

$$\tau_E = \frac{W}{P} = \frac{3}{P}\int n\,dv \int \frac{\int Q\,dv'}{n\chi V'}\,dx = \frac{3a^2}{4\bar{\chi}} \qquad (1)$$

In the above expression Q(x) is the local heating rate where x denotes a non-dimensional plasma surface label and V′ is the derivative w.r.t. x of the volume V inside surface x. The expression is in general an integral equation and only in cases such as χ being independent of temperature T can simple derivations of $\bar{\chi}$ be made [25]. The definition (1) is the one we shall use in this paper to obtain a scaling of τ_E from that of $\bar{\chi}$.

It has been shown by Connor [21] that, with very minimal assumptions on the equations describing local transport, the scaling of the local diffusivity $\chi(x)$ can be derived for turbulent fluctuations characterized by frequencies $\omega \ll \Omega_{ci}$. Such turbulent fluctuations are described by the non-linear ion gyro-kinetic equation [26]. In reference [27] the scaling of χ is derived from the application of the Connor-Taylor scale invariance technique [20]. This scaling has the following form for turbulence characterized by scale lengths $\lambda \sim \rho_i$ (the ion Larmor radius)

$$\chi_S = \rho^2 \frac{V_{th}}{L}\; F_S\left(\frac{\nu L}{V_{th}}, \beta, q, \varepsilon, \kappa, \frac{L_j}{L_k}\right) \qquad (2)$$

Long wavelength turbulent fluctuations characterized by scale lengths $\lambda \sim L$ (e.g. minor radius) give the scaling

$$\chi_L = \rho v_{th}\ F_L\left(\frac{\nu L}{v_{th}}, \beta, q, \varepsilon, \kappa, \frac{L_j}{L_k}\right) \qquad (3)$$

The parameters of Eqs.(2) and (3) are as follows : v_{th} a thermal velocity, ν a collision frequency, β a local plasma beta, q the local safety factor, $\varepsilon = ax/R$, κ the flux surface elongation and L_j and L_k denote additional scale lengths like shear length L_S, $L_n = (\nabla n/n)^{-1}$, $L_T = (\nabla T/T)^{-1}$ etc. Both Eqs.(2) and (3) consist of a leading term and some function F whose arguments are dimensionless. The interpretation of the leading term in (2) is that of a step length of the diffusive processes which is of order ρ and a timescale of order L/v_{th} ; for Eq.(3) the step length is of order L and the time scale is the $E \times B$ drift time or the Bohm time. Eqs.(2-3) are very general and permit a vast number of possible scalings through permutations of the variables ρ_e, ρ_i, ν_{ei}, ν_{ee}, ν_{ii} . Expression (2) has recently been used [22] in a local transport analysis of data from JET ICRF heated plasmas with sawtooth-free periods (monsters).

In order to derive scaling laws for τ_E we choose the following definitions for the parameters entering Eqs.(2-3)

$$\rho = \rho_\theta = \frac{2\pi a m v_{th}}{e\mu_0 I} \quad , \quad \frac{v_{th}}{L} = \frac{v_{th}}{a} \quad , \quad \nu_* = \frac{\nu R}{v_{th}} \quad , \quad \beta = \beta_I \qquad (4)$$

In Eqs.(4) ρ_θ is the poloidal Larmor radius and β_I is poloidal beta; the toroidal β_ϕ or the ratio between β and a stability value β_{crit} are other possible choices for β , but since F contains q and ε they are all equivalent to $\beta = \beta_I$. The choice of L as respectively a (with v_{th}) and R (with ν) is arbitrary since the aspect ratio ε enters F. The definition of ν_* should also include $q\varepsilon^{-3/2}$ but no appropriate spatial average of this quantity is available. The plasma parameters ρ_θ, ν, v_{th} in (4) all depend on local values of the temperature $T_e(x)$ or $T_i(x)$ .The latter two are replaced by an appropriate average temperature defined as

$$T = \frac{W}{6\pi^2 e n a^2 \kappa R} \qquad (5)$$

in which n is the volume averaged density. We substitute Eq.(5) into i (4), Eq.(4) into (3) and (2), insert for $\bar{\chi} = \chi_S$ or $\bar{\chi} = \chi_L$ in (1) and solve for τ_E . This gives the *short* wavelength scaling of τ_E

$$\tau_E = \tau_{ES}\ F_S^{-2/5}\ ,\ \tau_{ES} = C_S\ a\ I^{4/5}\ (\frac{a\kappa R\ n}{P})^{3/5}\ ,\ F_S = F_S(\nu_*, \beta, q, \varepsilon, \kappa) \quad (6)$$

and the *long* wavelength scaling of τ_E

$$\tau_E = \tau_{EL}\ F_L^{-1/2}\ ,\ \tau_{EL} = C_L\ a\ I^{1/2}\ (\frac{a\kappa R\ n}{P})^{1/2}\ ,\ F_L = F_L(\nu_*, \beta, q, \varepsilon, \kappa) \quad (7)$$

Both scaling expressions include a leading term τ_{ES} or τ_{EL} and a function F. The dependence of τ_E upon F is weaker than it is for χ upon F . The exponents in Eqs.(6-7) for minor-major radius arise from the choices of L in (4). Different values for these exponents in the leading terms (6-7) may emerge from an inter-machine data analysis; neither minor radius a or major radius R have been varied significantly in the JET data. The leading term τ_{ES} given by Eq.(6) corresponds to the "Lackner" or plateau scaling law given in [18] . The arguments of F are the global parameters

$$\nu_* = C_1\ \frac{a^4\ R^3\ \kappa^2\ n^3}{W^2}\ ,\quad \beta = \beta_I = \frac{8W}{3\mu_0\ R\ I^2}$$

$$q = q_{cyl} = \frac{2\pi a^2 \kappa B}{\mu_0 R I}\ ,\ \varepsilon = \frac{a}{R}\ ,\ \kappa = \frac{b}{a} \quad (8)$$

The constants C_S , C_L and C_1 in Eqs.(6-8) can *only* be determined if an association of ρ_θ , ν and v_{th} with ions or electrons is made. If we choose $\rho_\theta = \rho_{i\theta}$, $v_{th} = v_i$ and $\nu = \nu_{ei}$ then we get

$$C_S = (\frac{9\pi\sqrt{6}\ \mu_0^2\ e^2}{8 m_p^{1/2} A^{1/2}})^{2/5} = 9.44\ 10^{-15}\ A^{-1/5}\ \ [V^{3/5} s A^{-1/5} m^{-2/5}]$$

$$C_L = (\frac{9\pi\mu_0\ e}{4})^{1/2} = 1.19\ 10^{-12}\ \ [V^{1/2} s m^{-1/2}] \quad (9)$$

$$C_1 = 3\sqrt{2}\ \pi^{5/2}\ e^4\ Z_{eff}\ \frac{\log \Lambda_{ei}}{\varepsilon_0^2} = 2.033\ 10^{-50}\ [A^2 V^2 s^2 m^2]$$

The dependence upon A, the ion-proton mass ratio, is very weak for the leading term in the short wavelength scaling while in the long wavelength scaling there is no A dependence. For C_1 we have fixed the coulomb logarithm at 16 and Z_{eff} at

2. If the dimensionless parameters are associated with the electrons then m_e will replace m_p in the expression for C_S and the mass ratio A will be excluded. For the results presented in this paper A=2 is assumed since only JET data with deuterium as the main and injected gas has been used.

3. Preparation and interpretation of JET data

Results from JET experiments recently surveyed in [28] include data from several different operational scenarios as regards additional heating and plasma configuration. We concentrate on two categories of data obtained during the period 1986-89. The first category comprises ELM-free H-mode confinement data from NBI heated plasmas with an internal separatrix. The second category is made up of data from NBI and ICRF heated plasmas attached to toroidal limiters. The data required for the scaling laws (6-7) is the volume averaged density measured by a FIR interferometer (no profile fitting) and a, R, κ determined from magnetic analysis. The total thermal energy data is prepared from diamagnetic measurements (W_{dia}) and from MHD fits to magnetic data (W_{MHD}) as follows. Both are related to the total stored thermal energy W via

$$W_{dia} = W + \frac{3}{2} W_{fi\perp}$$

$$W_{MHD} = W + \frac{3}{4} W_{fi\perp} + \frac{3}{2} W_{fi\parallel}$$

in which subscript fi refers to the fast ion components where the latter are due to minority ions (mainly perpendicular component) accelerated by ICRH and ions injected by NBI (nearly isotropic for JET). The fast ion energy component can be expressed in the form $W_{fi} = P\tau_s /2$, where τ_s is the slowing down time. A separate analysis has given the following approximate fits

$$W_{fiNBI} = 0.11\ 10^{19} \frac{P_{NBI}}{n} \qquad (10a)$$

$$W_{fiICRH} = 1.90\ 10^{13} \frac{P_{ICRH}\, T_e^{3/2}}{n} \qquad (10b)$$

The fits are then used to calculate the thermal energy W from Tthe measurements. The values calculated from W_{dia} agree with those obtained from W_{MHD} and in this paper data from W_{dia} is presented.

Table I summarizes the variation of the key parameters in the H-mode data set. It can be seen that τ_E varies more than one order of magnitude as do τ_{ES} and τ_{EL} . On the other hand ν_* varies by nearly four orders of magnitude and any dependence of τ_E upon ν_* must therefore be weak. In order to demonstrate the variation of τ_E with the leading terms of Eq.6 or 7 it is essential to examine data for which the arguments of the function F are approximately constant. Figures 1a to 1d show the L and H-mode data plotted as $\log(\tau_E)$ against $\log(\tau_{ES})$ and $\log(\tau_{EL})$. The data in the plots has been selected for two ranges of collisionality $0.001 < \nu_* < 0.002$ and $0.005 < \nu_* < 0.01$ and for two ranges of plasma beta

$$0.3 < \beta < 0.5 \text{ and } 0.5 < \beta < 1.1 \text{ (H-mode data)}$$
$$0.1 < \beta < 0.3 \text{ and } 0.3 < \beta < 1.1 \text{ (L-mode data)}$$

Four symbols are used in the Figures corresponding to the above ranges. The dotted lines in the Figures arise from linear regression fits to each of the collisionality regimes. These lines have slopes of 1 in Figure 1a (H-mode data) and Figure 1c (L-mode data) for the short wavelength scaling given by Eq.(6). In contrast the long wavelength scaling comparison produces slopes of 1.4 to 1.5; it therefore does not fit the data. The difference between the slopes for the long and the short wavelength scaling laws is diminished if the fast ion energy content (Eqs.10) is not subtracted from the measured W_{dia} and W_{MHD} . The data clearly reveals the "banded" variation (via ν_*) of τ_E with the leading term τ_{ES} . Each band corresponds to a range of ν_* and the structures seen in Figures 1a to 1d indicates a dependence of F upon ν_* .

4. The F function

A simple representation of F which is also used in [21,27] is

$$F(\nu_*, \beta, q, \varepsilon, \kappa) = \nu_*^{\alpha} \ \beta^{\gamma} \qquad (11a)$$

This expression for F will lead to the commonly used power law representation of τ_E as a function of n, I, P etc. However other forms of F are equally well possible, e.g. an off-set linear representation of τ_E as a function n, I, P etc. such as the Rebut-Lallia form [10]

$$F = \nu_*^{1/2} \ \beta^{-1/2} \ (1 - 0.033 \ \frac{q^{1/2}}{\kappa^{1/2}\varepsilon^{5/12}} \ \nu_*^{1/4} \beta^{-1/2}) \qquad (11b)$$

We now examine the variation of F predicted by the various theoretical transport models. These models have quite complex forms for F usually involving L_s, L_n and L_T but for our purposes we shall use Eq.(11a) in the following. The values of α and γ are listed in Table II for the theories considered in [21] and [34] . The predictions of these theoretical models can be compared with the data on F derived from Eq.(6). For convenience we define via Eq.(6) the following function

$$f_S = F_S^{-2/5}(\nu_*, \beta, q, \varepsilon, \kappa) = \frac{\tau_E}{\tau_{ES}} \qquad (12)$$

Figures 2a and 2b show JET H-mode data values of f_S derived from (12) plotted vs ν_* and vs β respectively. Figure 2a shows that f_S decreases with ν_* and that this decrease can be represented by any of the theoretical models in Table II that has a non-negative value of α . Turbulence driven transport via DTEM or DTIM can therefore be discarded as the resulting scaling has the wrong ν_* dependence. The β dependence of f_S is more difficult to establish since in the data β exhibits a relatively small variation. Figure 2b suggests that there is no apparent variation with β; indeed it is difficult to distinguish any variation to within $-0.4 < \gamma < 0.4$ corresponding to slopes in Figure 2b of +0.16 and -0.16 respectively. Therefore some weak β dependence such as that of the resistive fluid turbulence theory cannot be ruled out. A few of the theoretical scaling laws listed in Table II are shown as dotted lines in Figure 2a. The solid line represents the best fit to the data and corresponds to $\alpha = 0.4$. This result is the same as that found in local transport studies [22] in which data could be fitted for values of γ ranging from -1 to -0.3 in the outer half of the plasma. A recent study of local transport in TFTR [35] has also shown that calculated values of χ_i and χ_e both increase with ν_* while the variation with β appears to be less certain.

On the basis of these investigations we cannot select one single theoretical model as the best representation of the data. However a *combination* of models may seem more plausible, e.g. collisionless trapped electron mode or η_i modes in the central and middle regions and resistive fluid turbulence in the edge region. Such a combination of theoretical models would explain both the variation of F with ν_* seen in Figure 2a and the spatial variation of F , i.e. γ , found in [22] .

5. Similarity of existing scaling laws

In this section we shall examine the similarity between 15 existing Tokamak scaling laws [5-18] We insert the expressions (8) in Eq.(11a), substitute for F in Eq.(6) and solve for τ_E . The result is an expression of the power law form

$$\tau_E \;=\; C_E\, a^{y1}\, \kappa^{y2}\, R^{y3}\, n^{y4}\, I^{y5}\, P^{y6}\, q^{y7} \qquad (13)$$

in which the exponents y1 to y6 become functions of α and γ ; the safety factor q is also included and will be used below. The constant C_E depends on C_S (or C_L) and C_1 etc. Table III lists the expressions for the exponents y1 to y6 in terms of α and γ . We could have also proceeded from Eq.(11b) to derive a generic expression for τ_E in the off-set linear form but the algebra becomes much more involved.

Some of the scaling laws [5-18] are already in the form (13); for others which employ the off-set linear representation we examine only the term that describe the additional heating. In addition the scaling laws may depend on magnetic field B, ion to proton mass ratio A and Z_{eff} . We ignore the latter two dependencies since Z_{eff} appears in Eq.(9) and scaling with A is only based on A = 1 and A = 2 data. The safety factor q is used to replace B by the current I as Eq.(13) does not contain B explicitly. Table IV presents the actual values of the exponents y1-y7 assigned to the 15 scaling laws when they are put in the form of Eq.(13). A scan of the Table values shows that these laws are *apparently* quite different.

To express each scaling law in the gyro-reduced from (6) we need to replace the dependence of F_S on the four variables I, n, P and L (either R or a) by $\nu^{*}\beta^{y}$. With just two free parameters α and γ it is not possible to put any given scaling law in this form exactly. However if we allow for small changes δ_k to the exponents listed in Table IV then we can obtain the nearest equivalent dimensionally correct scaling law. We minimise the sum of the squares of the differences between the actual exponents (Table IV) and those corresponding to the nearest dimensionally correct form. Each scaling law is then expressed as (L is either a or R)

$$\tau_E = \tau_{ES}\; F_S^{-2/5} \quad L^{\delta 1}\, n^{\delta 2}\, I^{\delta 3}\, P^{\delta 4} \qquad (14)$$

where the quantity δ^2 , which is minimised, is the sum of the squares of the residuals δ_k and is given by

$$\delta^2 \;=\; \frac{1}{4} \sum_{k=1}^{4} \delta_k^2$$

The minimisation of δ^2 yields the values of α and γ that are listed in Table V. It can be seen that the residual δ is generally quite small and probably within the error bounds of the exponents of Table IV.

The variation of F with ν_* , i.e. α , for all the existing laws, except the last two, is similar to the variation seen in Figure 2a; since several of the scaling laws are based on data from smaller Tokamaks the dependence of F upon ν_* is therefore the same on these as it is on JET. In Figure 3 we show the variation of f_S with ν_* at approximately constant β for both the JET L-mode (β =0.25) and H-mode data (β =0.35). The JET data is accompanied by the predictions of the ASDEX [14] , Mirnov [15] , Shimomura [16] scaling laws shown as dotted curves for both the L and H-mode data. The dashed curve corresponds to the Kaye-Goldston scaling law [8] and the solid curve represents the Rebut-Lallia scaling law [10] expressed by Eq.(11b) for β =0.35. The curve for the off-set linear law (Rebut-Lallia) can hardly be distinguished from the curve of the ASDEX-Mirnov-Shimomura power laws especially when errors on W are taken into account.

Both the L and H-mode data in Figure 3 have f_S decreasing with ν_* but the H-mode data has higher numerical values of f_S. This implies that the transport in the bulk of the Tokamak plasma is the same; however in the edge region the turbulence in the H-mode is at a lower level than in the L-mode.

From Table V we notice that three scaling laws, "Rebut-Lallia" , "Merezhkin" and "Lackner" (plateau scaling) are rigorously dimensionally correct while two laws "Kaye-big" and "T10" are approximately dimensionally correct. However the "Merezhkin" and "T-10" scaling expressions do not fit the JET data. The remaining scaling laws all have $0.37 < \alpha < 0.54$ and $-0.5 < \gamma < 0.6$ which is similar to the best fit of Figure 2a and to the result found in [22] . The similarity between the scaling laws is brought out by the variation with ν_* rather than that with β . In summary all of the scaling laws which give a reasonable fit to the data have a similar variation with collisionality ν_* and it is the variation with β that leads to the large multiplicity of scaling laws.

For completeness we have also repeated the above procedure for the long wavelength turbulence form given by Eq.(7); the values of α, γ and δ are given in Table VI. The results are not too different from those obtained for the short wavelength scaling but the range for α is narrower ($0.22 < \alpha < 0.39$) and that for γ is broader ($-0.44 < \gamma < 0.94$). One other point to notice from Table VI is that the residual δ is very small for both the Goldston [5] and the Neo Kaye [11] scaling laws.

6. Ohmic scaling and constraints

The ohmic power input is expressed as

$$P_{OH} = R_\phi I^2 \ , \ R_\phi = \eta_{\phi\phi} \frac{2R}{a^2 \kappa} \ , \ \eta_{\phi\phi} \approx \eta_\parallel$$

$$\eta_\parallel = \frac{C_\eta}{T^{3/2}} \ , \ C_\eta = \frac{m_e^{1/2} e^{1/2} Z_{eff} \log \Lambda_{ei}}{3 \varepsilon_0^2 (2\pi)^{3/2}}$$

Experimental values of P_{OH} can be derived from analysis of magnetic data. This involves a model for the plasma internal inductance ℓ_i and its time derivative. In practice this estimate for P_{OH} turns out to be too inaccurate to allow for comparisons between ohmic τ_E data and the scaling laws of section 2. Instead we compare ohmic data on the stored energy W with the product $P_{OH}\tau_{ES}$. Provided the time derivative dW/dt is negligible compared with P_{OH} we can insert Eq.(5) for T to get the equation linking P to W

$$P_{OH} = C_{OH} \ a \ \kappa^{1/2} R^{5/2} n^{3/2} I^2 W^{-3/2} \ , \ C_{OH} = 2C_\eta (6\pi^2 e)^{3/2} \qquad (15)$$

Expression (15) can then be used to eliminate P from the scaling law Eq.(6). The result is the short wavelength scaling for ohmic plasmas

$$W_S^{OH} = C_S^{OH} \ a^{5/4} \kappa^{1/2} R \ n^{3/4} I \ F_S^{-1/4} \qquad (16)$$

This particular scaling has also been derived in [10] The numerical value of the constant in Eq.(16) is evaluated for $Z_{eff} = 2$ and $\log \Lambda_{ei} = 16$

$$C_S^{OH} = C_S^{5/8} C_{OH}^{1/4} = 1.847 \ 10^{-16} \ [Vs \ ]$$

We can again use the representation Eq.(11a) for the function F to derive power law expressions similar to Eq.(13) for ohmic plasmas. The relationship between the exponents y1 to y5 in terms of the parameters α and γ are for completeness listed in Table III.

From a large amount of JET ohmic data obtained during 1988 (approximately 10000 sets of data) we have selected data which satisfies the following steady state constraints

$$\frac{dW_B}{dt} < 0.1\ [MW]\ , \quad \frac{dW}{dt} < 0.1\ P_{OH}$$

where W_B denotes the poloidal field energy. The above restrictions yield appr. 800 data values of $W = W_{DIA}$. Figure 3 shows how this data fits the scaling given by W_S^H and we have included actual JET data on Z_{eff} (visible bremsstrahlung measurements) in the definition of C_{OH} rather than the number 2 used for the numerical value given.

7. The scaling of the "fusion product" by similarity techniques

We can obtain a scaling for the fusion product $nT\tau_E$ by using Eqs.(6) or (7). The scaling represents an appropriate *global* value of this product since it includes the volume averaged density, the temperature defined by (5) and the global confinement time. The axial value of the fusion product will of course be somewhat larger than the global value. For additionally heated plasmas the short wavelength turbulence scaling results in

$$(n\,T\,\tau_E)_S = \frac{C_S^2}{6\pi^2 e}\ a^{6/5}\,\kappa^{1/5}\,R^{1/5}\,n^{6/5}\,I^{8/5}\,F_S^{-4/5}\,P^{-1/5} \qquad (17a)$$

There is a weak dependence of this product with power P. The ohmic case gives

$$(n\,T\,\tau_E)_S^{OH} = \frac{(C_S^{OH})^{7/2}}{C_{OH}\,6\pi^2 e}\ a^{11/8}\,\kappa^{1/4}\,n^{9/8}\,I^{3/2}\,F_S^{-7/8} \qquad (17b)$$

The highest axial value of this product obtained on JET (#20981) is

$$(n_D\,T_i\,\tau_E)_{measured}^{axial} = 8\,10^{20}\quad [m^{-3}\,keV\,s\,]$$

This value has been achieved in double null separatrix plasma configurations exhibiting H-mode confinement. The measurements show that the high value of the fusion product is achieved transiently for a period of 0.3-0.4 seconds. During such a transient period the net input power of 18MW (NBI) is reduced to 10MW because the time derivative of W reaches 8MW. For L-mode confinement we use JET pulse 20367 with a limiter plasma and both NBI and ICRH. These two pulses both have a high fusion performance and represent the two different

modes of operation in JET. We now use the data to make extrapolations to the reactor regime.

As reactor parameters we choose those given by the ITER team in the design study [36] . Table VII lists all principal parameters for JET pulse 20981 (H-mode confinement), JET pulse 20367 (L-mode confinement) and for ITER the L-H mode analogues. We apply a similarity technique in the extrapolation in the sense that both confinement modes in ITER have values of the arguments ν_* and β which are similar to their JET counterparts hence the values of F obtained on JET in the two pulses are used for ITER. The advantage of using a similarity technique is that it avoids the uncertainty in τ_E associated with the β dependence of F. Furthermore the similarity technique eliminates the need to make a choice between an off-set linear scaling law [9,10,17] and a power law [5,7,8,11-16] both of which have been widely used to characterize the dependence of τ_E with input power P. As emphasized earlier the function F embodies both these forms.

The implications of the similarity technique are as follows. We must adjust the input power P and average plasma density from the values quoted in reference [36] to maintain the same collisionality ν_* and β . The quoted ITER values for elongation κ and the safety factor q_{cyl} lie outside the range explored in JET experiments. In order to make an acceptable extrapolation from the two JET pulses we therefore assume an ITER value of q_{cyl} of 2.42. This means that the plasma current is 17MA instead of 22MA. The results of the extrapolation from JET to ITER are also given in Table VII. The L-mode operation of ITER with the parameters given should therefore yield sub-ignition performance with a $Q_{thermal}$ of order 1 whereas H-mode operation of ITER should establish a $Q_{thermal}$ slightly above the ignition threshold. In deriving $Q_{thermal}$ we have assumed that the profiles of n and T obtained in ITER are the same as the analogue JET pulses; this assumption should be guaranteed by the use of the similarity technique.

8. Conclusion

In this paper we have studied that scaling of the confinement time which arises from thermal transport in a turbulent plasma. The scaling is expressed by a leading term which characterises the turbulence length scale and a function F describing the source of the turbulence. Two limits have been considered: a short and a long wavelength limit, each limit denoting that wavelength at which the energy loss dominates. A one order of magnitude variation in JET confinement data is found to be well described by the short wavelength or gyro-reduced Bohm scaling. The long wavelength or Bohm scaling does not fit the data.

The uncertainty in the variation of the function F with β makes it very difficult to precisely identify the physical mechanisms which account for the observed transport in a Tokamak. However, because F is observed to increase with ν_* , theoretical models such as DTEM which predict a strong decrease of F with ν_* can be eliminated. Of the remaining theoretical models, collisionless drift waves, the η_i mode or resistive fluid turbulence, no single model is a particularly good fit to the data but within the error bounds of the analysed data they are all possible candidates. A combination of models, e.g. the η_i mode in the inner region of the Tokamak and resistive fluid turbulence in the outer region would also be a possible explanation of the observed scaling.

We have shown that the multiplicity of existing scaling laws may be approximately expressed as the gyro-reduced scaling with different forms for the function F. All the scaling laws have essentially the same dependence of F upon ν_* but they have different dependencies upon β ; the latter is the reason why they appear to be so different when expressed in terms of I, n, P etc. In this sense we conclude that the "gyro-reduced Bohm" scaling constitutes *a unified physical scaling law* for Tokamak energy confinement.

Finally we have shown how a similarity technique can be employed to predict the L and H-mode confinement time and fusion product in ITER by using the values of the function F from two high performance JET L and H-mode pulses. This technique eliminates the need to make a choice about the β dependence of F and the type of scaling law (off-set linear or product law) and hence improves the accuracy of the predictions.

Acknowledgements

The authors would like to acknowledge useful discussions with J. Connor, J. DeBoo and M.N. Rosenbluth on aspects of the dimensional analysis contained in this paper. The authors thank P. Lallia for helpful comments on the manuscript and finally they thank the JET team for making the data available for analysis.

Parameter	UNITS	Minimum	Maximum
a	m	0.92	1.19
R	m	2.87	3.25
κ		1.34	1.91
n	$10^{20}m^{-3}$	0.04	0.88
I	MA	1	5
P	MW	2.1	23.8
W	MJ	0.45	11.1
τ_E	s	0.1	1.8
W_S	MJ	0.21	2.72
τ_{ES}	s	0.036	0.327
W_L	MJ	0.0146	0.2
τ_{EL}	s	0.0032	0.0214
ν_*		10^{-5}	0.1
β		0.05	1.11
f_S		3.18	6.56
f_L		19	149
q_{cyl}		1.65	4.50

Table I. Ranges in JET H-mode data for parameters used in scaling law studies. The parameters are defined in the text.

Theory	α	γ	Reference
Collisonal drift wave	0,1/3,2/3,1	0	23,29
Collisionless trapped electron mode	0	0	23,29,32
Dissipative trapped electron mode	-1,-2	0	23,29,31
Dissipative trapped ion mode	-1	0	23
η_i mode	0	0	23,32,33
Overlapping islands	0	0	34
Resistive fluid turbulence	1	-1	21
Res. fluid turbulence (electrostatic)	1	0	21

Table II. Theoretical scaling laws for the confinement time τ_E which can be derived as Eq.(6) with the function F_S given by Eq.(12) as $F = \nu^{*} \ \beta^{\gamma}$. Some values of α are taken from Table 5 of [21] .

Exponent	Short wave	Long wave	OH Short wave	OH Long wave
y1 (a)	$8-8\alpha$	$6-8\alpha$	$17-16\alpha-2\gamma$	$13-16\alpha-2\gamma$
y2 (κ)	$3-4\alpha$	$2-4\alpha$	$6-8\alpha-\gamma$	$4-8\alpha-\gamma$
y3 (R)	$3-6\alpha+2\gamma$	$2-6\alpha+2\gamma$	$-5\alpha-5\gamma$	$-5\alpha-5\gamma$
y4 (n)	$3-6\alpha$	$2-6\alpha$	$3-9\alpha-3\gamma$	$2-9\alpha-3\gamma$
y5 (I)	$4+4\gamma$	$2+4\gamma$	$4+8\alpha+6\gamma$	$1-8\alpha+6\gamma$
y6 (P)	$-3+4\alpha-2\gamma$	$-2+4\alpha-2\gamma$	-	-
Denominator	$5-4\alpha+2\gamma$	$4-4\alpha+2\gamma$	$8-4\alpha+2\gamma$	$7-4\alpha+2\gamma$

Table III The dependency of the exponents y1 to y6 in Eq.(13) upon the parameters α and γ is expressed as the ratio between a numerator listed in the Table and a denominator given in the bottom line. The short and long wavelength scalings have also been applied to ohmic scaling which includes the constraint on power P and τ_E (Eq.15).

Scaling law	a	κ	R	n	I	P	q	Ref
Rebut-Lallia	1	0.5	0.5	0	1	0	0	10
ASDEX	0	0	1	0	1	0	0	14
Mirnov	1	0.5	0	0	1	0	0	15
Shimomura	-1	-0.5	2	0	1	0	1	16
Odajima	2	1	0	0	0	0	0	9
Kaye big	0.2	-0.05	0.8	0.1	1.15	-0.5	0.3	12
Kaye all	-0.3	-0.05	1.15	0.1	1.15	-0.5	0.3	12
Kaye-Goldston	-0.5	0.25	1.65	0.25	1.25	-0.58	0.09	8
Goldston	-0.38	0.5	1.75	0	1	-0.5	0	5
Neo Kaye	-0.04	0.28	1.3	0.14	1.12	-0.59	0	11
Resistive MHD	1.5	0.5	0.5	0.5	0.5	-0.5	0	17
Lackner	0.4	1	1.8	0.6	0.8	-0.6	0.4	18
T-10	0.92	0.38	1.92	1	0.33	-0.4	0.76	13
Merezhkin	0	0.416	3	1	0	-0.33	0.66	7
Alcator	1	0	2	1	0	0	1	6

Table IV. Tokamak scaling laws for auxiliary heated Tokamaks cast in the form

$$\tau_E = C\, a^{\nu 1}\, \kappa^{\nu 2}\, R^{\nu 3}\, n^{\nu 4}\, I^{\nu 5}\, P^{\nu 6}\, q^{\nu 7}$$

Some scaling laws [9,10,13,17] also include an ohmic term. All the table values except the last one refer only to the auxiliary heating term or to the term for incremental confinement time.

Scaling law	α	γ	δ
The authors	0.4	-0.4 to 0.4	0
Rebut-Lallia	0.5	-0.5	0
ASDEX	0.54	-0.49	0.056
Mirnov	0.54	-0.49	0.056
Shimomura	0.54	-0.49	0.056
Odajima	0.42	-0.8	0.108
Kaye big	0.47	0.13	0.068
Kaye all	0.49	0.25	0.132
Kaye-Goldston	0.28	0.58	0.132
Goldston	0.44	0.2	0.1
Neo Kaye	0.37	0.55	0.08
Resistive MHD	-	-	-
Lackner	0	0	0
T-10	-0.02	-0.82	0.044
Merezhkin	0	-1	0
Alcator	0.19	-1.18	0.072

Table V. The Tokamak scaling laws for auxiliary heated Tokamaks recast to match the short wavelength scaling given by Eq.(14). The parameter δ is the residual in the exponents of Eq.(13) required to make the scaling laws dimensionally correct (see text).

Scaling law	α	γ	δ
Rebut-Lallia	0.35	-0.14	0.06
ASDEX	0.39	-0.12	0.076
Mirnov	0.39	-0.12	0.076
Shimomura	0.39	-0.12	0.076
Odajima	0.272	-0.44	-0.08
Kaye big	0.324	0.61	0.076
Kaye all	0.345	0.74	0.136
Kaye-Goldston	0.222	0.94	0.124
Goldston	0.285	0.565	0.06
Neo Kaye	0.225	0.914	0.02
Resistive MHD	0.5	0.25	0
Lackner	-	-	-
T-10	-0.17	-0.454	0.104
Merezhkin	0	-1	0
Alcator	0.044	-0.71	0.096

Table VI. The Tokamak scaling laws for auxiliary heated Tokamaks recast to match the long wavelength scaling formally given by Eq.(14) with subscripts S replaced by L. The parameter δ is the residual in the exponents of Eq.(13) required to make the scaling laws dimensionally correct (see text).

Param.	UNITS	JET L-mode	JET H-mode	ITER L-mode	ITER H-mode
B	T	3.1	2.9	4.9	4.9
I	MA	5.2	4.1	17	17
a	m	1.1	1.1	2.15	2.15
κ		1.6	1.8	2.2	2.2
R	m	3	3	6	6
n	$10^{20}m^{-3}$	0.28	0.28	0.5	0.56
P	MW	11.9	10.5	100	54
q_{cyl}		2.25	2.42	2.42	2.42
β		0.17	0.41	0.20	0.43
ν_*		$1.5\ 10^{-3}$	$5.4\ 10^{-4}$	$1.6\ 10^{-3}$	$6.6\ 10^{-4}$
f_S		2.24	5.04	2.24	5.04
W	MJ	5.43	9.34	187	349
τ_E	s	0.46	0.90	1.87	6.45
$nT\tau_E$	$10^{20}m^{-3}$keVs	0.40	1.35	6.60	39
$Q_{thermal}$		0.1	0.3	1.4	∞

Table VII. Scaling of parameters from JET L-mode pulse 20367 and H-mode pulse 20981 to ITER values. The plasma current has been changed from 22MA to 17MA to reproduce the JET value of the safety factor. In this extrapolation the arguments ν_* and β of the function F are held at values similar to those obtained in the two mentioned JET pulses. $Q_{thermal} = (P_\alpha + P_{neutron}) / (P - P_\alpha)$ where P_α and $P_{neutron}$ denote the power levels resulting from thermonuclear D-T reactions (thermal-thermal).

References

[1] GORBUNOV, E.P., MIRNOV, S.V., STRELKOV, V.S., Nucl. Fusion 10(1970)43

[2] HUGILL, J., Nucl. Fusion 23(1983)331

[3] HUGILL, J., SHEFFIELD, J., Nucl. Fusion 18(1978)15

[4] PFEIFFER, W., WALTZ, R. E., Nucl. Fusion 19(1979)51

[5] GOLDSTON, R.J., Plasma Physics and Controlled Fusion 26(1984)87

[6] PARKER, R.R., Nucl. Fusion 25(1985)1127

[7] MEREZHKIN, V.G., MUKHOVATOV, V.S., Soviet Physics J.E.T.P. Letters 33(1981)446

[8] KAYE, S.M., GOLDSTON, R.J., Nucl. Fusion 25(1985)65
KAYE, S.M., Phys. of Fluids 28(1985)2327

[9] ODAJIMA, K., SHIMOMURA, Y., "Energy confinement scaling based on offset linear characteristics", JAERI-M 88-068, JAERI (March 1988)

[10] REBUT, P.H., LALLIA, P.P., WATKINS, M.L., Proc 12th Conf. on Plasma Physics and Controlled Fusion Research, Nice (1988), IAEA-CN-50/D-4-1

[11] KAYE, S.M., "Global energy confinement scaling in Tokamaks : new trends", Princeton Plasma Physics Laboratory Memorandum, Unpublished (November 1986)

[12] KAYE, S.M., "Survey of energy confinement scaling expressions", ITER specialist's Meeting, Garching (May 1988)

[13] T-10 GROUP, "Investigation of energy confinement in ECRH experiments on T-10", ITER specialist's Meeting, Garching (May 1988)

[14] GRUBER, O., Proc. Int. Conf. Plasma Physics, Lausanne, Switzerland, Vol.1 (1984)67, Commission of the European Communities

[15] STRELKOV, V.S., Nucl. Fusion 25(1985)1189

[16] SHIMOMURA, Y., "Empirical scaling of energy confinement of L-mode plasma and optimized mode and some consideration of reactor core plasma in Tokamak", JAERI-M87-080, JAERI (1987)

[17] CORDEY, J.G., BARTLETT, D.V., BHATNAGAR, V. et al., Proc. 11th Conf. on Plasma physics and Controlled Nuclear Fusion Research, Kyoto (1986) Vol. 1, IAEA, Vienna (1987) 99.

[18] LACKNER, K., GOTTARDI, N., Tokamak confinement in relation to plateau scaling, JET Report JET-P(88)77, submitted to Nucl. Fusion

[19] KADOMTSEV, B.B., Soviet J. Plasma Physics, 1(1975)295

[20] CONNOR, J.W., TAYLOR, J.B., Nucl. Fusion 17(1977)1047

[21] CONNOR, J.W., Plasma Physics and Controlled Fusion 20(1988)1047

[22] CHRISTIANSEN, J.P., CORDEY, J.G., MUIR, D.G., Nucl. Fusion 29(1989)1505

[23] DUCHS, D.F., POST, D.E., RUTHERFORD, P.H., Nucl. Fusion 17(1977)565

[24] BERLIZOV, A.B., BOBROVSKIJ, G.A., VASIN, N.L., VERTIPOROKH, A.N., et al, Proc 9th Conf. on Plasma Physics and Controlled Fusion Research, Baltimore (1982), Vol.2, p63. IAEA Vienna

[25] CALLEN, J.D., CHRISTIANSEN, J.P., CORDEY, J.G., THOMAS, P.R., THOMSEN, K., Nucl. Fusion 27(1987)1857

[26] FRIEMAN, E.A., CHEN, Liu, Phys. Fluids 25(1982)502

[27] HAGAN, W.K., FRIEMAN, E.A., Physics of Fluids 29(1986)3635

[28] BICKERTON, R.J. and The JET Team, Proc 12th Conf. on Plasma Physics and Controlled Fusion Research, Nice (1988), IAEA-CN-50/A-1-3

[29] WALTZ, R.E., DOMINGUEZ, R.R., WONG, S.K., DIAMOND, P.H. et al., Proc 11th Conf. on Plasma Physics and Controlled Fusion Research, Kyoto (1986), Vol.1, p345. IAEA Vienna

[30] TERRY, P.W., DIAMOND, P.H., Physics of Fluids 28(1985)1419

[31] CHEN, Liu, BERGER, R.L., LOMINADZE, J.G., ROSENBLUTH, M.N., Phys. Rev. Lett. 39(1977)754

[32] ROMANELLI, F., TANG, W.M., WHITE, R.B., Nucl. Fusion 26(1986)1515

[33] LEE, G.S., DIAMOND, P.H., Phys. of Fluids 29(1986)3291

[34] REBUT, P.H., BRUSATI, M., Proc. 10th Conf. on Plasma Physics and Controlled Fusion Research, Kyoto (1986) Vol.2, p.187.

[35] ZARNSTORFF, M.C., GOLDSTON, R.J., BELL, M.G., BITTER, M., et al. Controlled Fusion and Plasma Physics, Venice (1989) Vol.1, p.35.

[36] YUSHMANOV, P., TAKIZUKA, T., RIEDEL, K., KARDAUN, O., CORDEY, J.G., KAYE, S.M., POST, D.E., Preliminary Draft Report of the ITER L-mode scaling Working Group, ITER Confinement Working Session (August 1989)

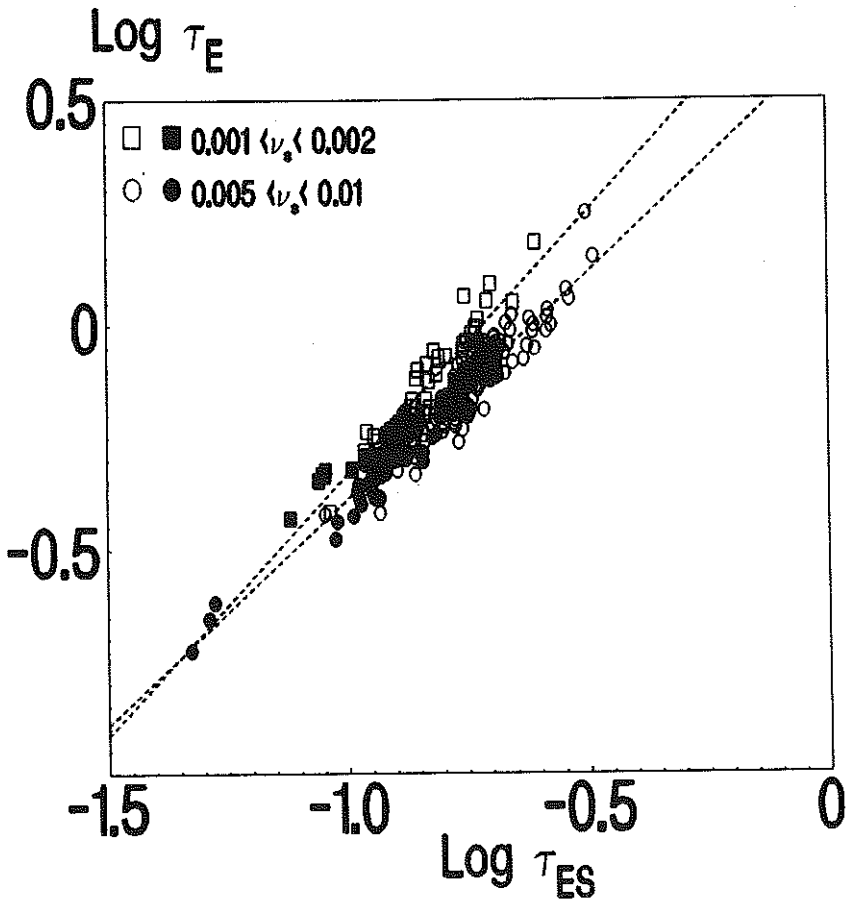

FIG. 1a. JET H-mode data on the confinement time versus the short wavelength scaling Eq.(6). Open symbols correspond to $0.3 < \beta < 0.5$ and for full symbols $0.5 < \beta < 1.1$

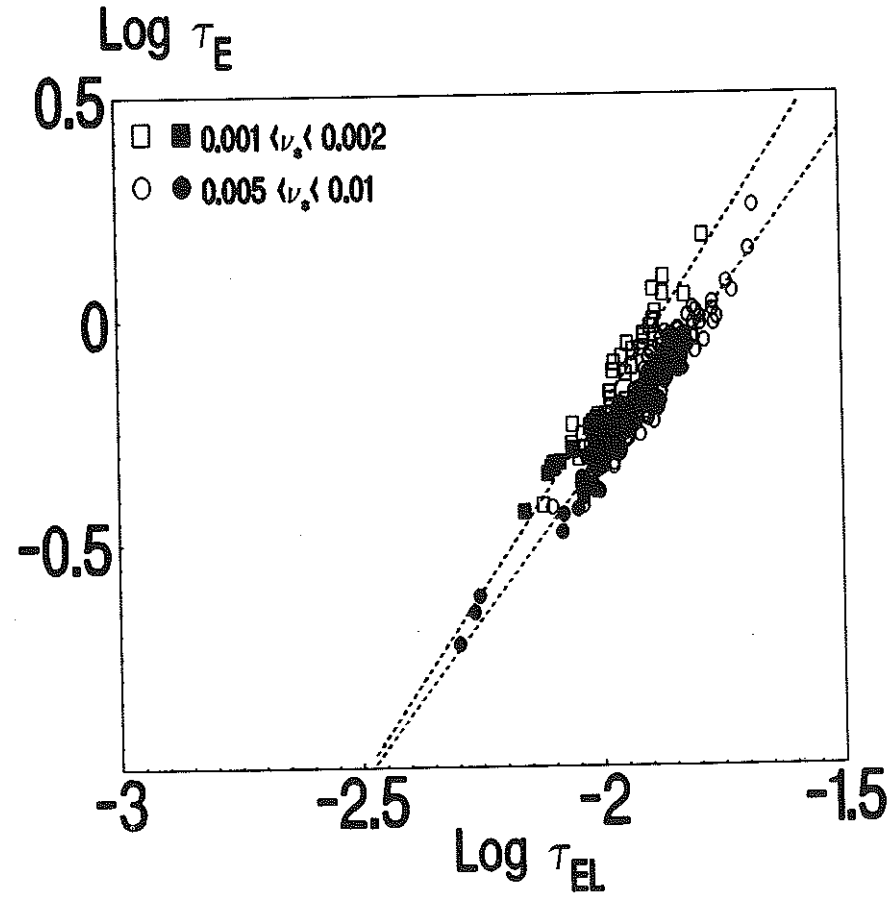

FIG. 1b. JET H-mode data on the confinement time versus the long wavelength scaling Eq.(7). Open symbols correspond to $0.3 < \beta < 0.5$ and for full symbols $0.5 < \beta < 1.1$

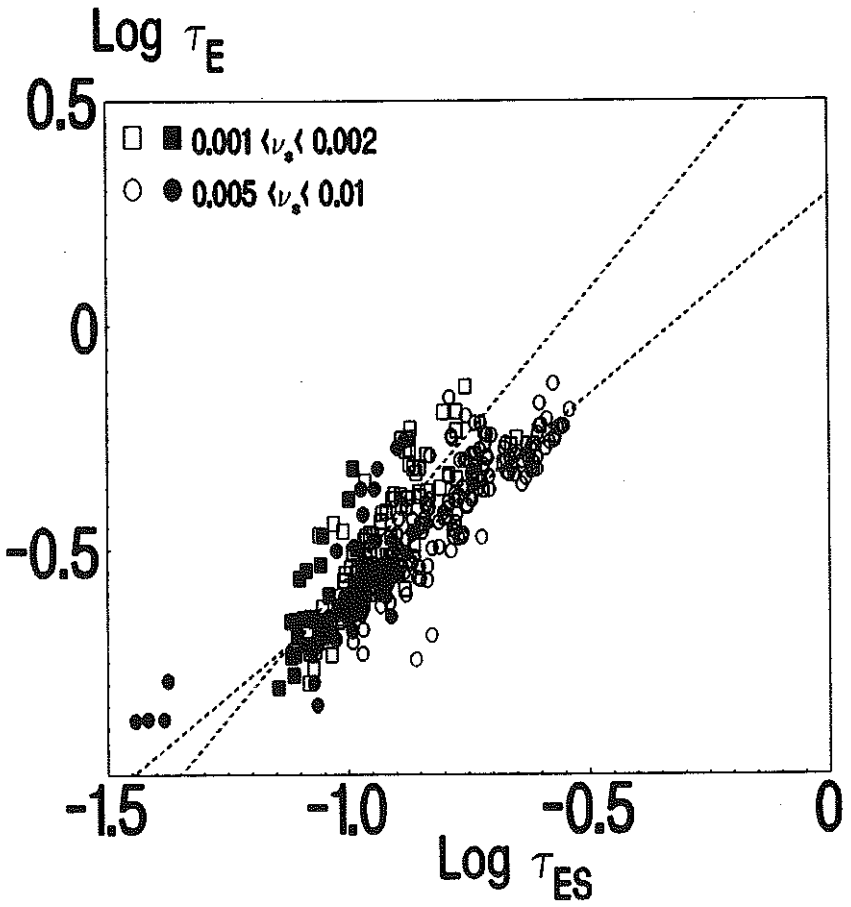

FIG. 1c. JET L-mode data on the confinement time versus the short wavelength scaling Eq.(6). Open symbols correspond to $0.1 < \beta < 0.3$ and for full symbols $0.3 < \beta < 1.1$.

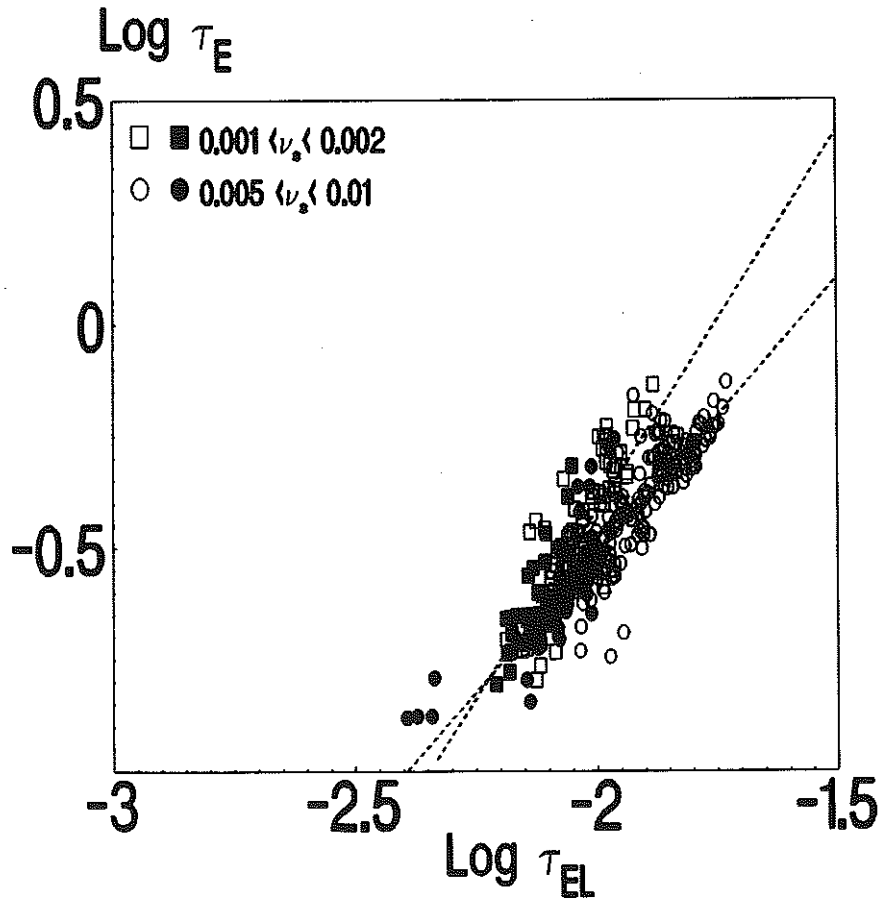

FIG. 1d. JET L-mode data on the confinement time versus the long wavelength scaling Eq.(7). The slopes of lines through the data are as in Figure 1b of order 1.5. The symbols have the same meaning as in Figure 1c.

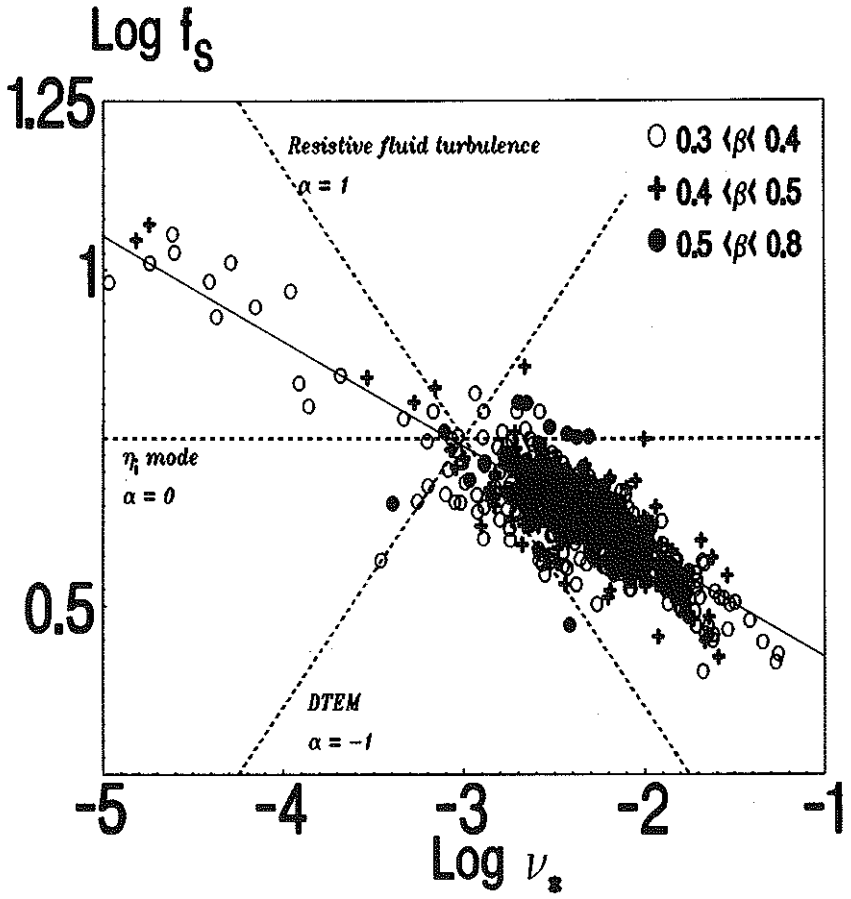

FIG. 2a. Variation of the function f_S (Eq.12) with ν_* for 3 ranges of β (H-mode data) and 3 theoretical scalings. Collisional drift waves have $1/3 < \alpha < 1$. The solid line arises from a linear fit to the data.

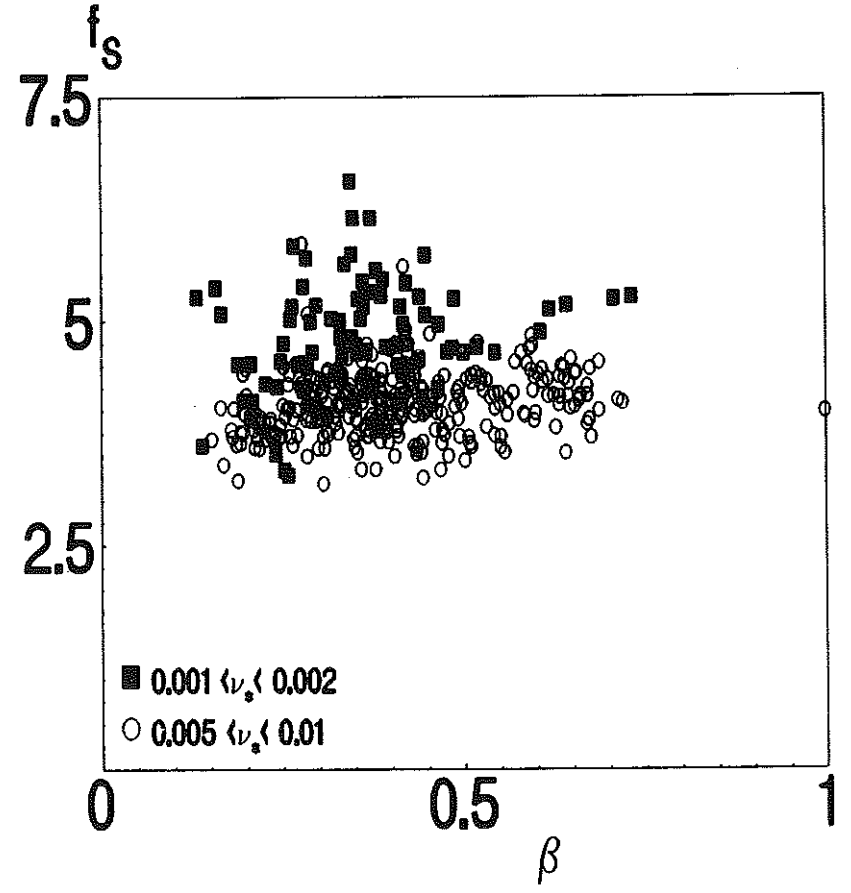

FIG. 2b. There is no apparent dependence of f_S (Eq.12) on β for JET H-mode data. The 'bands' of data points correspond to ranges of ν_* as depicted in Figure 2a

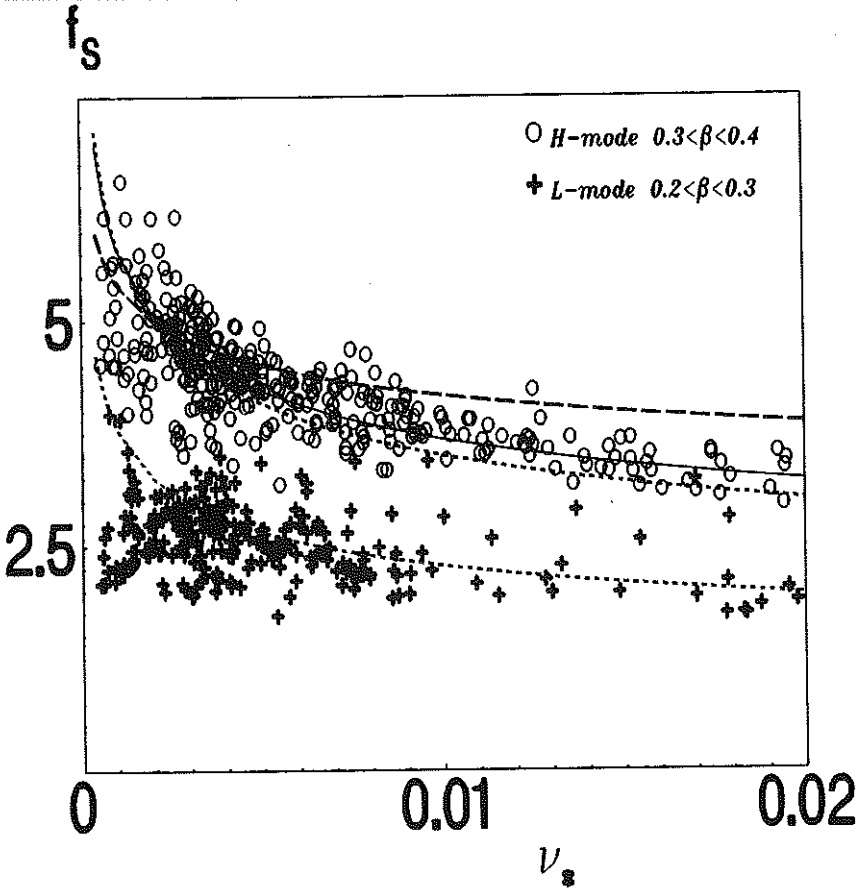

FIG. 3. Variation of the function f_S (Eq.12) with ν_s for JET L and H-mode data. The curves represent the scalings of [14-16] (dotted curves L and H-mode),[8] (dashed curve) and [10] (full curve).

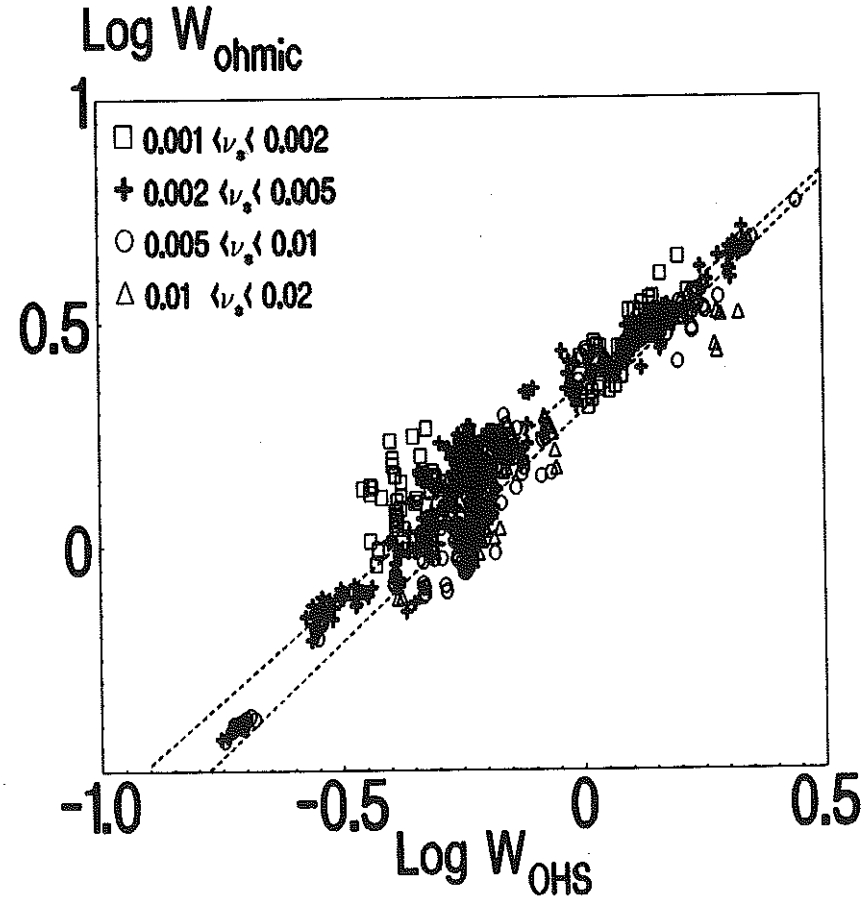

FIG. 4. Ohmic JET data for plasma energy versus the short wavelength scaling Eq.(16). Only steady state data is used as explained in the text. The variation with ν_s is similar to that seen in L and H-mode data. The dotted lines arise from linear fits to two collisionality groups of data.

APPENDIX 1.

THE JET TEAM

JET Joint Undertaking, Abingdon, Oxon, OX14 3EA, U.K.

J.M.Adams[1], F.Alladio[4], H.Altmann, R.J.Anderson, G.Appruzzese, W.Bailey, B.Balet, D.V.Bartlett, L.R.Baylor[24], K.Behringer, A.C.Bell, P.Bertoldi, E.Bertolini, V.Bhatnagar, R.J.Bickerton, A.Boileau[3], T.Bonicelli, S.J.Booth, G.Bosia, M.Botman, D.Boyd[31], H.Brelen, H.Brinkschulte, M.Brusati, T.Budd, M.Bures, T.Businaro[4], H.Buttgereit, D.Cacaut, C.Caldwell-Nichols, D.J.Campbell, P.Card, J.Carwardine, G.Celentano, P.Chabert[27], C.D.Challis, A.Cheetham, J.Christiansen, C.Christodoulopoulos, P.Chuilon, R.Claesen, S.Clement[30], J.P.Coad, P.Colestock[6], S.Conroy[13], M.Cooke, S.Cooper, J.G.Cordey, W.Core, S.Corti, A.E.Costley, G.Cottrell, M.Cox[7], P.Cripwell[13], F.Crisanti[4], D.Cross, H.de Blank[16], J.de Haas[16], L.de Kock, E.Deksnis, G.B.Denne, G.Deschamps, G.Devillars, K.J.Dietz, J.Dobbing, S.E.Dorling, P.G.Doyle, D.F.Düchs, H.Duquenoy, A.Edwards, J.Ehrenberg[14], T.Elevant[12], W.Engelhardt, S.K.Erents[7], L.G.Eriksonn[5], M.Evrard[2], H.Falter, D.Flory, M.Forrest[7], C.Froger, K.Fullard, M.Gadeberg[11], A.Galetsas, R.Galvao[8], A.Gibson, R.D.Gill, A.Gondhalekar, C.Gordon, G.Gorini, C.Gormezano, N.A.Gottardi, C.Gowers, B.J.Green, F.S.Griph, M.Gryzinski[26], R.Haange, G.Hammett[6], W.Han[9], C.J.Hancock, P.J.Harbour, N.C.Hawkes[7], P.Haynes[7], T.Hellsten, J.L.Hemmerich, R.Hemsworth, R.F.Herzog, K.Hirsch[14], J.Hoekzema, W.A.Houlberg[24], J.How, M.Huart, A.Hubbard, T.P.Hughes[32], M.Hugon, M.Huguet, J.Jacquinot, O.N.Jarvis, T.C.Jernigan[24], E.Joffrin, E.M.Jones, L.P.D.F.Jones, T.T.C.Jones, J.Källne, A.Kaye, B.E.Keen, M.Keilhacker, G.J.Kelly, A.Khare[15], S.Knowlton, A.Konstantellos, M.Kovanen[21], P.Kupschus, P.Lallia, J.R.Last, L.Lauro-Taroni, M.Laux[33], K.Lawson[7], E.Lazzaro, M.Lennholm, X.Litaudon, P.Lomas, M.Lorentz-Gottardi[2], C.Lowry, G.Magyar, D.Maisonnier, M.Malacarne, V.Marchese, P.Massmann, L.McCarthy[28], G.McCracken[7], P.Mendonca, P.Meriguet, P.Micozzi[4], S.F.Mills, P.Millward, S.L.Milora[24], A.Moissonnier, P.L.Mondino, D.Moreau[17], P.Morgan, H.Morsi[14], G.Murphy, M.F.Nave, M.Newman, L.Nickesson, P.Nielsen, P.Noll, W.Obert, D.O'Brien, J.O'Rourke, M.G.Pacco-Düchs, M.Pain, S.Papastergiou, D.Pasini[20], M.Paume[27], N.Peacock[7], D.Pearson[13], F.Pegoraro, M.Pick, S.Pitcher[7], J.Plancoulaine, J-P.Poffé, F.Porcelli, R.Prentice, T.Raimondi, J.Ramette[17], J.M.Rax[27], C.Raymond, P-H.Rebut, J.Removille, F.Rimini, D.Robinson[7], A.Rolfe, R.T.Ross, L.Rossi, G.Rupprecht[14], R.Rushton, P.Rutter, H.C.Sack, G.Sadler, N.Salmon[13], H.Salzmann[14], A.Santagiustina, D.Schissel[25], P.H.Schild, M.Schmid, G.Schmidt[6], R.L.Shaw, A.Sibley, R.Simonini, J.Sips[16], P.Smeulders, J.Snipes, S.Sommers, L.Sonnerup, K.Sonnenberg, M.Stamp, P.Stangeby[19], D.Start, C.A.Steed, D.Stork, P.E.Stott, T.E.Stringer, D.Stubberfield, T.Sugie[18], D.Summers, H.Summers[20], J.Taboda-Duarte[22], J.Tagle[30], H.Tamnen, A.Tanga, A.Taroni, C.Tebaldi[23], A.Tesini, P.R.Thomas, E.Thompson, K.Thomsen[11], P.Trevalion, M.Tschudin, B.Tubbing, K.Uchino[29], E.Usselmann, H.van der Beken, M.von Hellermann, T.Wade, C.Walker, B.A.Wallander, M.Walravens, K.Walter, D.Ward, M.L.Watkins, J.Wesson, D.H.Wheeler, J.Wilks, U.Willen[12], D.Wilson, T.Winkel, C.Woodward, M.Wykes, I.D.Young, L.Zannelli, M.Zarnstorff[6], D.Zasche[14], J.W.Zwart.

PERMANENT ADDRESS

1. UKAEA, Harwell, Oxon. UK.
2. EUR-EB Association, LPP-ERM/KMS, B-1040 Brussels, Belgium.
3. Institute National des Récherches Scientifique, Quebec, Canada.
4. ENEA-CENTRO Di Frascati, I-00044 Frascati, Roma, Italy.
5. Chalmers University of Technology, Göteborg, Sweden.
6. Princeton Plasma Physics Laboratory, New Jersey, USA.
7. UKAEA Culham Laboratory, Abingdon, Oxon. UK.
8. Plasma Physics Laboratory, Space Research Institute, Sao José dos Campos, Brazil.
9. Institute of Mathematics, University of Oxford, UK.
10. CRPP/EPFL, 21 Avenue des Bains, CH-1007 Lausanne, Switzerland.
11. Risø National Laboratory, DK-4000 Roskilde, Denmark.
12. Swedish Energy Research Commission, S-10072 Stockholm, Sweden.
13. Imperial College of Science and Technology, University of London, UK.
14. Max Planck Institut für Plasmaphysik, D-8046 Garching bei München, FRG.
15. Institute for Plasma Research, Gandhinagar Bhat Gujat, India.
16. FOM Instituut voor Plasmafysica, 3430 Be Nieuwegein, The Netherlands.
17. Commissiariat à L'Energie Atomique, F-92260 Fontenay-aux-Roses, France.
18. JAERI, Tokai Research Establishment, Tokai-Mura, Naka-Gun, Japan.
19. Institute for Aerospace Studies, University of Toronto, Downsview, Ontario, Canada.
20. University of Strathclyde, Glasgow, G4 ONG, U.K.
21. Nuclear Engineering Laboratory, Lapeenranta University, Finland.
22. JNICT, Lisboa, Portugal.
23. Department of Mathematics, Univeristy of Bologna, Italy.
24. Oak Ridge National Laboratory, Oak Ridge, Tenn., USA.
25. G.A. Technologies, San Diego, California, USA.
26. Institute for Nuclear Studies, Swierk, Poland.
27. Commissiariat à l'Energie Atomique, Cadarache, France.
28. School of Physical Sciences, Flinders University of South Australia, South Australia SO42.
29. Kyushi University, Kasagu Fukuoka, Japan.
30. Centro de Investigaciones Energeticas Medioambientales y Techalogicas, Spain.
31. University of Maryland, College Park, Maryland, USA.
32. University of Essex, Colchester, UK.
33. Akademie de Wissenschaften, Berlin, DDR.

CR 88.49.1A